



HAL
open science

A readily retrievable pool of synaptic vesicles

Yunfeng Hua, Raunak Sinha, Cora S Thiel, Roman Schmidt, Jana Hüve,
Henrik Martens, Stefan W Hell, Alexander Egner, Jurgen Klingauf

► **To cite this version:**

Yunfeng Hua, Raunak Sinha, Cora S Thiel, Roman Schmidt, Jana Hüve, et al.. A readily retrievable pool of synaptic vesicles. *Nature Neuroscience*, 2011, 10.1038/nn.2838 . hal-00650654

HAL Id: hal-00650654

<https://hal.science/hal-00650654>

Submitted on 12 Dec 2011

HAL is a multi-disciplinary open access archive for the deposit and dissemination of scientific research documents, whether they are published or not. The documents may come from teaching and research institutions in France or abroad, or from public or private research centers.

L'archive ouverte pluridisciplinaire **HAL**, est destinée au dépôt et à la diffusion de documents scientifiques de niveau recherche, publiés ou non, émanant des établissements d'enseignement et de recherche français ou étrangers, des laboratoires publics ou privés.

A readily retrievable pool of synaptic vesicles

Yunfeng Hua^{1,2*}, Raunak Sinha^{1,2*}, Cora S. Thiel^{1,2*}, Roman Schmidt³, Jana Hüve^{2,4}, Henrik Martens⁵,
Stefan W. Hell³, Alexander Egnér^{3,6}, Jurgen Klingauf^{1,2,4,7}

1- Dept. of Membrane Biophysics, Max-Planck Institute for Biophysical Chemistry, Am Fassberg 11, 37077 Goettingen, Germany.

2- Dept. of Cellular Biophysics, Institute of Medical Physics and Biophysics, University of Muenster, Robert-Koch-Str. 31, 48149 Muenster, Germany.

3- Dept. of NanoBiophotonics, Max-Planck Institute for Biophysical Chemistry, Am Fassberg 11, 37077 Goettingen, Germany.

4- Fluorescence Microscopy Facility Muenster, Center of Nanotechnology (CeNTech), Heisenbergstr. 11, 48149 Muenster, Germany.

5- Synaptic Systems GmbH, D-37079 Goettingen, Germany

6- present address: Laser-Laboratorium Goettingen e.V., Hans-Adolf-Krebs-Weg 1, 37077 Goettingen, Germany

* These authors equally contributed to this work.

7-Corresponding author:

Email: klingauf@uni-muenster.de

Tel.: +49(0)251 / 83-51001

Fax-: +49(0)251 / 83-55121

Although clathrin-mediated endocytosis (CME) is thought to be the predominant mechanism of synaptic vesicle (SV) recycling, it seems to be too slow for fast recycling. Therefore, it was suggested that a pre-sorted and pre-assembled pool of SV proteins on the presynaptic membrane might support a first wave of fast CME. In this study we monitored the temporal dynamics of such a 'readily retrievable pool' of SV proteins in rat hippocampal neurons using a novel probe. Applying cypHer 5, a new cyanine dye-based pH-sensitive exogenous marker, coupled to antibodies against luminal domains of SV proteins we could reliably monitor SV recycling and for the first time demonstrate the preferential recruitment of a surface pool of SV proteins upon stimulated endocytosis. Using fluorescence nanoscopy of surface labeled synaptotagmin 1, we could resolve the spatial distribution of the surface pool at the periaxial zone in hippocampal boutons, which represent putative sites of endocytosis.

A major rate-limiting step in synaptic transmission is the retrieval of SVs from the presynaptic membrane for further rounds of use. Several modes of SV retrieval have been proposed but the major pathway is considered to be CME^{1,2}. This process is relatively slow since post fusion the recycling machinery has to resort different vesicle membrane proteins in the right stoichiometry to generate fusion-competent SVs³. As a result this process occurs with a time constant of tens of seconds to minutes⁴. In order to sustain transmission during continuous activity, however, it was suggested that alternatively SVs 'kiss and run' with a time constant of 1 - 2 s, whereby the vesicles transiently fuse with the membrane without full collapse, hence retaining their molecular identity⁵⁻⁹.

The fast 'kiss and run' recycling mechanism not only would provide a kinetic advantage, but would spatially and temporally couple exo- and endocytosis. Using a GFP fusion protein with the coat-forming clathrin light chain, we previously found evidence that during the first 10 seconds of prolonged stimulation clathrin is not being recruited from the cytosol to form coated pits, although the rate of endocytosis measured with FM dyes is high³, suggesting that vesicles during this first phase are either retrieved by a clathrin-independent mechanism (kiss-and-run) or by preassembled coat structures at the periphery of the active zone.

Support for such 'readily retrievable pool' (RRetP) of preassembled structures came from experiments using fusion constructs of the SV proteins synaptobrevin 2 (Syb2) and synaptotagmin 1 (Syt1) with a pH-sensitive green fluorescent protein (GFP), pHluorin¹⁰. These studies showed that SVs post fusion lose their protein complement, and the molecular identity of SVs exocytosed and subsequently endocytosed is not conserved¹¹⁻¹³. Based on these observations we suggested that exocytosis and subsequent endocytosis are uncoupled and that there is a pool of preassembled vesicle proteins on the presynaptic surface that is preferentially retrieved on exocytosis^{3,13}. Previous studies using activity-dependent markers in snake neuromuscular terminals have proposed that the accumulation of such probes upon stimulation at the bouton margins might represent endocytic active zones^{14,15}. This is in agreement with other ultrastructural and high resolution microscopy analyses that describe the presence of several SV proteins

on the presynaptic membrane of resting synapses^{16,17}. Likewise the first reconstruction of the endocytic time course from electron micrographs of frog neuromuscular junctions quickfrozen at different times after stimulation revealed a first wave of CME lasting about 10 s¹⁸, in line with the notion of a pre-clustered pool being immediately available for a first wave of endocytosis upon stimulation¹³. Transient overexpression of the genetic exo-endocytic probe synaptopHluorin (spH)¹⁰, in which pHluorin is fused to the luminal domain of Syb2, in hippocampal boutons leads to targeting of up to ~30% of spH to the bouton membrane, constituting a surface pool that participates in SV protein recycling during compensatory endocytosis^{11,13}.

The finding, however, that expressed pHluorin-tagged versions of other SV proteins are found to only a minor extent on the surface - about 8% for synaptophysin-pHluorin² and even only about 2% for the glutamate transporter vGlut1-pHluorin¹⁹ - has called into question the existence of a surface pool of endogenous SV proteins. The high surface expression of spH and Syt1-pHluorin^{11,13} might be a mere overexpression artifact discrediting the use of pHluorins as optical probes for exo-endocytosis¹⁷. Endogenous SV proteins might be only transiently exposed to the surface during exo-endocytosis and might even remain clustered thereby tightly coupling exo- and endocytosis¹⁷. Thus, it is crucial to directly visualize spatially and temporally the retrieval of endogenous SV proteins from an RRetP of SVs, if it exists.

In this study we use a novel pH-sensitive fluorophore, cypHer5E^{20,21}, with a pH dependence opposite to that of pHluorin, coupled to antibodies against the luminal domains of Syt1 (α Syt1-cypHer) and the vesicular GABA transporter VGAT (α VGAT-cypHer²¹) - i.e. two endogenous SV proteins that, when overexpressed as pHluorin-tagged versions, either show very high or are expected to show very little surface expression respectively. By using these new probes in combination with spH¹⁰, we were able to visualize in real time the retrieval of endogenous Syt1 and VGAT from the surface RRetP of SVs¹³. The existence of an RRetP was further substantiated by 4Pi^{22,23} and isoSTED (isotropic stimulated emission depletion)²⁴ imaging of surface Syt1, which revealed a doughnut-like arrangement of Syt1 patches around the active zone and postsynaptic density complexes visualized by the cytomatrix at the active zone (CAZ) components RIM1/2 as well as the post-synaptic density (PSD) scaffolding protein Homer1. This is in

agreement with previous studies in *Drosophila melanogaster* neuromuscular junction and other synaptic preparations where endocytic 'hot spots' are located at the periaxial zone^{14,15,25-27}.

RESULTS

Monitoring exo-endocytosis of endogenous SV proteins

For characterizing the pH dependence of the fluorescence of cypHer-coupled antibodies, cultured hippocampal neurons were labeled with α Syt1-cypHer by incubation at 37°C for 3-4 hrs (**Material and Methods**), then fixed, permeabilized and superfused with buffers of different pH. The fluorescence was maximal at pH 5.5 and minimal at pH 9 (**Fig. 1a**). Normalized fluorescences ($\Delta F/F$) could be fit by a Henderson-Hasselbalch equation (**Fig. 1a**), yielding a pK_a value of 7.05, ideal to measure pH changes during exo- and endocytosis²⁸.

For measuring presynaptic activity, we labeled live hippocampal neurons with either α Syt1-cypHer or α VGAT-cypHer as above (**Fig. 1b**). During vesicle recycling these antibodies bind to their specific epitopes and are internalized (**Fig. 1c**). In the acidic vesicular lumen, protonated cypHer molecules emit red fluorescence, when excited at 640 nm, while cypHer-tagged molecules on the presynaptic membrane are sufficiently quenched at pH 7.4, leading to a punctate staining. Since spontaneous action potentials (APs) were not blocked during labeling, antibody uptake into SVs was primarily mediated by spontaneous activity. To assess the efficiency of this labeling strategy we stained neurons with α Syt1-cypHer by eliciting 900 APs at 20 Hz, a stimulus shown to deplete the entire recycling pool of SVs in hippocampal boutons²⁹. Neurons were then incubated at 37°C for 5-10 min followed by extensive washing to remove unbound antibodies. We next estimated the internalized fraction of cypHer for both staining protocols by quenching their fluorescence with NH_4Cl (50 mM) which equilibrates the pH across all membranes and therefore unmask any cypHer inside acidic compartments²⁹. This quenchable fraction, which represents the amount of α Syt1-cypHer internalized into SVs, is comparable for both staining protocols (**Supplementary Fig. 1**). The stimulation-independent procedure with long incubation time (3-4 hrs), however, labels a larger fraction of SVs (**Supplementary Fig. 1**). We next tested the efficiency of this probe to report stimulation-dependent exo-endocytosis. Trains of APs were evoked by electric field stimulation at 20 Hz, resulting in a rapid decay of cypHer fluorescence at individual boutons due to

quenching of vesicular cypHer upon fusion at the external pH of 7.4 (**Fig. 1d**). After cessation of stimulation cypHer-coupled antibodies are retrieved by compensatory endocytosis and dequenched during reacidification of the vesicle lumen (**Fig. 1e**). Interestingly, inhibitory boutons labeled by α VGAT-cypHer showed near-identical stimulation-dependent fluorescence transients for different stimulus strengths (**Fig. 1f**). CypHer labeling provides a reverse fluorescence signal in comparison to spH, as expected from its reverse pH sensitivity. However, the cypHer dye shows less photostability than spH, making correction for photo-bleaching necessary (**Supplementary Fig. 2; Material and Methods**) when not using a back-illuminated charged coupled device.

Size of the surface pool of SV constituents

As for spH, cypHer fluorescence changes scale with the stimulus strength for both α Syt1-cypHer and α VGAT-cypHer labeled boutons (**Fig. 1e,f**). The peak fluorescences, however, report the net difference between the kinetics of exo- and endocytosis during stimulation. But previous studies based on spH have shown that the initial rate of endocytosis post stimulus is similar to the endocytic rate during the stimulus period^{29,30}. Thus, we could estimate the pure exocytosis amplitude ΔF by back-extrapolating a linear fit to the initial post-stimulus rate of endocytosis (**Fig. 2a**). Back-extrapolated ΔF values, proportional to numbers of released SVs, rise linearly with stimulus strength (**Fig. 2b**) as shown previously for spH^{29,30}.

Up to ~30% of over-expressed spH is stranded on the synaptic membrane upon overexpression in hippocampal boutons^{12,13,29}. It has been shown, however, that endogenous SV proteins also are present on the membrane^{16,17}. To re-address this issue we superfused α Syt1-cypHer-labeled boutons with buffer of pH 5.5 to selectively visualize the presynaptic surface pool (**Fig.2c,d**). The size distribution of surface fluorescences from individual boutons was well fit with a Gaussian (adjusted $R^2 = 0.98$) with a mean of 49.46 ± 1.56 a.u. The size of this total surface pool corresponds to a fluorescence change induced by ~70 APs (**Fig. 2d inset**). This indicates that the surface pool might be capable of supporting compensatory endocytosis of SVs for stimuli of up to 70 APs i.e. it is similar in size to the readily releasable pool (RRP) of docked and primed vesicles³¹⁻³³.

Labeled antibodies report same recycling kinetics as spH

Next we labeled hippocampal neurons overexpressing the genetically encoded pH sensor spH with the cypHer-coupled antibodies and performed dual-color imaging. Because of the wide spectral separation no bleed-through was observed. Functional spH-expressing boutons were colabeled with α Syt1-cypHer (**Fig. 3a**). Since, the spH transfection efficiency is only ~10% not all α Syt1-cypHer-stained boutons co-express spH. We next examined the fluorescence changes in response to 200 APs at 20 Hz (**Fig. 3a**). SpH and α Syt1-cypHer responses of the same boutons showed mirror-image signals with near-identical endocytic time constants for monoexponential fits (~23 s versus ~22 s). This indicates that both reporters - an overexpressed and an exogenous probe - reliably report exo-endocytosis and do not artificially affect SV recycling. Next, we labeled spH-transfected boutons using the marker for GABAergic synapses (**Fig. 3b**). A fraction of ~32% of all spH-expressing boutons could be stained with α VGAT-cypHer representing the fraction of inhibitory synapses in our cultures. Stimulation with 200 APs at 20 Hz induced similar fluorescence transients (~22 s exponential endocytic time constant) in both channels (**Fig. 3b**). Therefore, the kinetics of endocytosis and reacidification in inhibitory synapses are indistinguishable from the whole population response as probed with spH and α Syt1-cypHer.

A readily retrievable surface pool of SV constituents

Previous studies have shown that SV proteins are also resident on the bouton membrane and that these surface proteins actively participate in endocytic recycling resulting in molecular non-identity of vesicles exo- and endocytosed by the same stimulus^{11,13}. However, it has not been possible so far to directly study the kinetics of this functional surface pool with an optical tracer that selectively labels the native proteins. By engineering a Tobacco Etch Virus (TEV)-cleavage site between the vesicle protein Syb2 and pHluorin, however, the fluorescence of surface spH could be eliminated by TEV digest and its participation in recycling shown indirectly¹³. Thus, we labeled spH-TEV transfected neurons with α Syt1-cypHer or α VGAT-cypHer and incubated them with TEV protease for 15 min¹³, to silence the non-vesicular surface spH-TEV fluorescence while keeping α Syt1-cypHer unperturbed. Next we elicited 50 APs at 20 Hz, a stimulus shown to deplete the RRP of docked vesicles in hippocampal boutons^{31,32}. An increase in

fluorescence was observed in the spH trace followed by little or no recovery (**Fig. 4a** above) indicating that instead of freshly exocytosed SV constituents cleaved surface spH-TEV was preferentially retrieved¹³. Is this preferential uptake of membrane spH a mere overexpression artifact due to surface-stranded spH or does it represent a specific retrieval mechanism? The fluorescence transient in the simultaneously recorded cypHer channel, which labels endogenous Syt1 in the same SVs, showed unperturbed fluorescence recovery implying that endocytosis and reacidification of SVs were normal (**Fig. 4a** below). This shows that SV proteins are endocytosed, but are derived from a functional surface pool^{13,34}.

Using spH-TEV, however, we were not able to directly visualize and prove the retrieval from the surface pool. Now, using cypHer, displaying a pH-dependence opposite to spH, we could perform the reverse experiment. We selectively silenced most of the vesicular cypHer fluorescence in spH-transfected boutons by photobleaching at 640 nm for 5 min. To minimize photobleaching of surface α Syt1-cypHer we transiently bathed neurons in extracellular buffer of pH 8.5. Stimulation with 50 APs at 20 Hz induced typical fluorescence spH transients (**Fig. 4b** top), but prebleaching the vesicle pool abolished most of the exocytic fluorescence decrease of the cypHer signal during stimulation (**Fig. 4b** bottom). Notably, after stimulation onset the cypHer fluorescence increases and reaches a plateau which demonstrates the retrieval of non-bleached cypHer-labeled Syt1 molecules from the presynaptic membrane. This reaffirms the existence of an RRetP of presorted SV constituents on the presynaptic membrane which are preferentially endocytosed on exocytosis, a pool we termed previously 'easily retrievable pool'³. Note, that a slight delay or even small downward dip in the cypHer traces is fully explained by incomplete bleaching of the vesicular fluorescence resulting in some remaining contribution of exocytosis. Because the cypHer surface fluorescence even at pH 8.5 is reduced only less than tenfold, it would be significantly bleached when attempting to fully bleach the vesicular fraction by longer bleaching times. Next we tested whether such RRetP also exists for other SV proteins like VGAT which has been shown to be present only in very low copy numbers in SVs³⁵. We repeated the same experiment using spH-transfected neurons co-stained with α VGAT-cypHer (**Fig. 4c**) revealing that even for low copy number SV proteins there exists a surface pool which is preferentially recycled by the endocytic machinery.

To rule out that spH overexpression might have altered the targeting of SV proteins to the vesicular and surface pools, we repeated the above experiments using only exogenous cypHer reporters (**Fig. 4d,e**). Both, kinetics and amplitude of cypHer transients were comparable to the dual-color recordings, showing that compensatory endocytosis of Syt1 or VGAT is not perturbed by spH overexpression and primarily draws upon a functional pool of SV constituents on the presynaptic membrane.

We next compared the size of the RRP, i.e. the fluorescence drop on 50 APs (**Fig. 4a**, bottom) to that of the RRetP, i.e. the cypHer fluorescence increase on 50 APs after vesicular cypHer bleaching (**Fig. 4d,e**). The estimated mean size of the RRP was 40.2 ± 6.9 a.u. for α Syt1-cypHer and 34.8 ± 3.6 a.u. for α VGAT-cypHer (**Fig 4f**) whereas the mean RRetP size turned out to be only 19.5 ± 6.2 a.u. for α Syt1-cypHer and 17.7 ± 2.1 a.u. for α VGAT-cypHer. These smaller size estimates of the RRetP might be solely attributed to partial bleaching of the surface pool. Thus, to avoid prebleaching we attempted to preferentially stain the surface Syt1 pool (cf. **Fig. 2c**). Neurons were briefly incubated with saturating concentration of α Syt1-cypHer in the presence of TTX for 5 min. Again, when stimulated with 50 APs at 20 Hz (**Fig. 5**; 1st Stim.), the fluorescence signal increased to a plateau as in the vesicular cypHer bleaching experiments in **Fig. 3**. Now the fluorescence increase, a measure of the RRetP was 53.7 ± 4.8 a.u. (**Fig. 4f**), quite similar to the measured RRP size (**Fig. 4a**). Thus, the RRP appears to be counterbalanced by an RRetP of similar size.

Reuse of SVs from the RRetP on sequential stimulation

Can SV recycled from the RRetP be re-released on repeated stimulation? To answer this question a second bout of stimulation to surface Syt1-labeled boutons was applied 60 s later (**Fig. 5**). The cypHer fluorescence responses indeed now displayed a fast drop due to partial exocytosis of previously recycled RRetP components followed by an endocytic increase. Released fractions were $27.6 \pm 5.1\%$ for 50 APs and $49.7 \pm 9.2\%$ for 200 APs in very good agreement with similar experiments using FM styryl dyes as tracers³⁶. However, somewhat unexpected, the endocytic increases for the second stimulus clearly exceeded the exocytic drops. This could be due to incomplete depletion of the RRetP during the first 50 AP stimulus (cf. **Supplementary Fig. 3**), but more likely is due to partial replenishment of the RRetP after

the first stimulus by exocytosed vesicles that had taken up cyHer by spontaneous recycling during the initial labeling phase.

Spatial organization of the RRetP

How is the functional surface pool spatially organized at the presynapse? To address this we used the same antibody, α Syt1, to specifically label the surface pool. After labeling at 4 °C, we fixed the cells immediately and identified synapses by colabeling with antibodies against *bona fide* CAZ or PSD proteins. The spatial organization of the Syt1 surface pool was investigated using dual-color isoSTED²⁴ nanoscopy. In the three-dimensional reconstruction of hippocampal *en passant* boutons from isoSTED image stacks (**Fig. 6a-c**), we find distinct Syt1 patches in the vicinity of the active zones.

From a large list of antibodies against CAZ elements, we obtained good signal-to-noise ratio only for antibodies against RIM1/2. The observed antibody fluorescence distribution was rather broad (**Fig. 6a**), extending up to 1 μ m along its long axis. While large active zone sizes have been documented in hippocampal synapses in EM sections (680 nm)³³ as well as in recent full 3D EM reconstructions³⁷, the even larger patches seen in our experiment indicate that active zone sizes are indeed overestimated by labeling the large RIM proteins at the N-terminal Zn finger domain.

In order to provide an additional fingerprint of synapses, we modified our staining by targeting the PSD opposing the active zone with antibodies against Homer1. This introduced a characteristic spatial separation between the two channels (**Fig.6b**). We analyzed the distribution of the Syt1 patches with respect to Homer1 in each of the three bouton regions (**Fig. 6c**) as depicted in the histograms (**Fig. 6d**). Mean distances between Syt1 and Homer1 increase as the azimuth angle α between the estimated orientation of the axon (**Fig. 6b**, arrows) and Syt1-Homer1 connecting vectors approaches 0 and $\pm \pi$ respectively, due to a higher probability to include Syt1 patches that are localized adjacent on the axolemma but are not associated with Homer1. At other angles, the observed distances are smaller and reach minimum distances of about 100-300 nm for a bouton (**Fig. 6d**). This finding agrees well with a localization analysis of a large number of synapses in 4Pi microscopy^{22,23} image stacks (**Fig. 6e** and

Supplementary Fig. 4). Together with our *in vivo* imaging data we therefore suggest that the associated Syt1 patches constitute the preassembled RRetP.

DISCUSSION

We have devised a new technique to measure stimulation-dependent exo-endocytosis in hippocampal presynaptic boutons. Using cypHer-conjugated antibodies against Syt1 and VGAT we achieved specific labeling of endogenous vesicle proteins. Antibody uptake into SVs during the 3-4 hrs incubation at 37°C, however, might be mediated to a large degree by spontaneous recycling, and thus might label a different SV pool in comparison to stimulation-induced uptake³⁸⁻⁴⁰. But analysis of spontaneous and evoked recycling using α Syt1-cypHer revealed that both modes of release draw on a common pool of SVs at these central synapses⁴¹. The good spectral separation between cypHer and spH allowed us to use both pH-dependent optical reporters in tandem resulting in two independent read-outs of presynaptic activity. AP-driven fluorescence transients of α Syt1-cypHer and α VGAT-cypHer-stained boutons exhibited mirror-image transients in comparison to spH due to the opposite pH-dependence of cypHer fluorescence. Kinetics of endocytosis and reacidification assayed by both methods, however, were nearly identical showing that this cypHer-based approach reliably monitors recycling of endogenous SV proteins.

By fluorescently silencing the surface spH we could clearly demonstrate the molecular non-identity of vesicle proteins exo- and endocytosed as previously shown¹³. But the unaffected cypHer fluorescence transient enabled us for the first time to monitor the endocytosis of SV derived from the RRetP consisting of cleaved spH and endogenous Syt1 labeled with α Syt1-cypHer. To provide direct evidence that this surface pool actively participates in exo-endocytosis we photobleached the vesicular cypHer signal from α Syt1-cypHer and α VGAT-cypHer stained boutons and elicited 50 APs previously shown to deplete the RRP. The then-observed increase in cypHer fluorescence, in parallel to the spH fluorescence decay, demonstrates preferential endocytosis of cypHer-stained Syt1 and VGAT residing on the bouton membrane. This preferential recruitment of surface SV proteins on stimulation was not affected by spH overexpression, thus validating our and others' previous pHluorin-based results^{11,13}. Although overexpression of some pHluorin fusion proteins leads to an excess of surface-stranded proteins, it has been shown to not affect the functional size of this pool^{11,13}. The size of this RRetP could be determined

by selective dequenching of surface-bound α Syt1-cypHer with brief pulses of acidic buffer. We found that retrieval from the RRetP could counterbalance exocytosis for up to 70 APs at 20 Hz. We further measured the size of this functional surface pool by preferentially staining surface Syt1 and monitoring its endocytosis, which yielded comparable estimates. Thus the RRetP has a capacity similar to the RRP. This is also corroborated by the nanoscopy of surface-stranded Syt1 at the periaxial zone, generally identified as the site of endocytosis^{14,15,25,42}, which revealed several preassembled patches, from which new SVs could bud. Moreover it is interesting to note that even for the low copy number protein VGAT, there is a functional surface pool that is preferentially internalized upon stimulated exo-endocytosis, raising the question whether this transporter can be active in the plasma membrane.

Our findings demonstrate the existence of a functional RRetP of native vesicle constituents like Syt1 and VGAT at the peri-active zone. The preferential uptake of vesicle constituents from a surface pool nicely explains the molecular non-identity of SVs exo- and endocytosed. Although overexpression of spH may lead to a significant increase of the total surface pool, the cypHer experiments clearly show the existence of an endogenous SV protein surface pool participating in SV recycling. Existence of a RRetP can nicely explain the first wave of CME observed in the first reconstruction of the endocytic time course from electron micrographs of frog neuromuscular junctions¹⁸. Also, it can explain why the initial endocytic rate remains constant irrespective of the stimulation strength as suggested in other studies^{29,30}. However, once this RRetP is depleted at ~70 APs, the rate drops since the endocytic machinery has to invest more energy and time to recapture and resort freshly exocytosed components to the sites of retrieval. Since endocytosis of the RRetP (**Fig. 4**) itself, however, takes a number of sec's, the main advantage of an RRetP might not be so much a gain in speed but rather a gain in precision of resorting and recluster to ensure maximum fusion competence of newly endocytosed vesicles. This is in line with the counter-intuitive finding that knock-down or knock-out of major sorting factors like AP-1 and AP-2 subunits result in similar or even faster endocytic kinetics of a large fraction of retrieved SV proteins^{43,44}, probably corresponding to bulk endocytosis. However, the re-availability of endocytosed SVs is slowed down and their fusion competence diminished⁴⁴.

In three recent studies the importance of Ca^{2+} for coupling of exo- and endocytosis is emphasized⁴⁵⁻⁴⁷. Work in *Drosophila melanogaster* suggests that there might be a vesicular Ca^{2+} channel that once incorporated into the plasma membrane by fusion would allow Ca^{2+} entry at the site of endocytosis and thus might trigger the retrieval from the RRetP⁴⁷. However, the detailed mechanism that couples exocytosis from the RRP and compensatory endocytosis from the RRetP and the molecular underpinnings remain to be elucidated.

Supplementary Information is available on the Nature Neuroscience website.

ACKNOWLEDGEMENTS

We thank Michael Pilot and Ina Herfort for the preparation of primary cell cultures of hippocampal neurons, Erwin Neher and Robert H. Chow for critical reading of the manuscript. We acknowledge Daniel Boening and Magalie Martineau for experimental support and we are grateful to Kirill Kolmakov and Vladimir Belov for providing us with the new fluorescent dye KK114. We would also like to thank Mrinalini Hoon and Nataliya Glyvuk for useful suggestions. This work was supported by grants from the ESF/DFG (EUROMEMBRANE programme, EuroSynapse CRP FP-020 to J.K. :) as well as from the DFG (KI 1334/1-1 to C.S.T. and J.K., SFB 944 to J.K., CMPB to, A.E. and S.W.H., SFB755 to A.E. and S.W.H.). Y.H. is supported by a stipend from the Max-Planck foundation and R.Sin. is supported by a stipend from the International Max Planck Research School in Neurosciences at the University of Goettingen.

AUTHOR CONTRIBUTIONS

Y.H., R.Sin. and C.S.T. conducted the majority of the experiments. J.H. collected and analyzed the 4Pi microscopy data. IsoSTED microscopy and analysis was performed by R.S. and A.E. in the department of S.W.H. H.M. synthesized the cypHer-conjugated antibodies. J.K. conceptualized the project and together with Y.H. and R.Sin. designed the experiments. R.Sin. and J.K. wrote the paper with the help of Y.H. and C.S.T. All authors discussed the results and commented on the manuscript.

FIGURE LEGENDS

Figure 1. CypHer-coupled antibodies are a reliable tool to measure stimulation-dependent exo-endocytic cycling of endogenous vesicle constituents.

(a) Average normalized fluorescence of α Syt1-cypHer-stained hippocampal boutons from multiple trials (each trial consisted of >30 boutons) as a function of pH. The solid curve is a fit to a Henderson–Hasselbalch equation (adjusted $R^2 = 0.99$) yielding a pK_a of 7.05. Error bars represent s.d.

(b) Schematic depicting fluorescence changes of cypHer during exo-endocytosis. CypHer-coupled antibodies (red dots) bind to the extracellular domain of vesicular proteins (Syt1 or VGAT) and remain quenched due to the neutral extracellular pH. During endocytosis and reacidification, however, the cypHer fluorescence is dequenched. Re-exocytosis upon stimulation results in quenching of the cypHer fluorescence at the extracellular neutral pH.

(c) Fluorescence image of hippocampal neurons labeled with α VGAT-cypHer shows a punctate pattern with puncta typically representing individual boutons.

(d) Fluorescence images of hippocampal neurons stained with α VGAT-cypHer before and after application of 900 APs and 100 s later.

(e) Average normalized fluorescence transient of α Syt1-cypHer stained boutons in response to different AP trains at 20 Hz ($n = 3$ experiments with > 50 boutons for each). Traces were corrected for photobleaching. Error bars represent s.e.m.

(f) Average normalized fluorescence transient of α VGAT-cypHer stained boutons in response to different AP trains at 20 Hz ($n = 3$ experiments with > 50 boutons for each). Traces were corrected for photobleaching. Error bars represent s.e.m.

Figure 2. Dose-response curve to analyze the size of the surface pool.

(a) Averaged fluorescence transients of α Syt1-cypHer-stained boutons in response to 50, 100 and 200 APs at 20 Hz ($n = 5$ experiments with > 50 boutons for each). Lines were fit to the initial fluorescence recovery phases to estimate the endocytic rate constant during stimulation. Back-extrapolation to zero yields the exocytosis amplitudes. Error bars represent s.e.m.

(b) Average peak changes in fluorescence (ΔF) plotted as a function of AP number (filled circles) together with ΔF values corrected for endocytosis during stimulation (triangles) by back-extrapolation (a). These data points lie close or on a line fit.

(c) Average fluorescence response to an acid pulse of boutons labeled with α Syt1-cypHer yielding the size of the surface pool. Error bars represent s.e.m.

(d) Distribution of bouton fluorescence responses to an acid pulse. The solid black line is a Gaussian fit (adjusted $R^2 = 0.99$) yielding a mean size of 49.46 ± 1.56 a.u. Inset, mean size of the surface pool estimated by the acid pulse is equivalent to the absolute fluorescence change triggered by 70 APs.

Figure 3. Comparison of vesicle recycling kinetics probed with synaptopHluorin and cypHer-coupled antibodies.

(a) Top: Staining of spH-transfected hippocampal neurons with α Syt1-cypHer. Fluorescence images show colocalisation of individual boutons expressing spH (green) with endogenous Syt1 (red) labeled with α Syt1-cypHer. Bottom: Average fluorescence transients of double-labeled boutons in response to 200 APs at 20 Hz ($n = 5$ experiments with > 50 boutons for each). Traces were corrected for photobleaching. Error bars represent s.e.m. Scale bar, 5 μ m.

(b) Top: Staining of spH-transfected hippocampal neurons with α VGAT-cypHer. Fluorescence images show colocalisation of individual boutons expressing spH (green) with the inhibitory synapse marker VGAT (red). Bottom: Average fluorescence transients of double-labeled boutons in response to 200 APs

at 20 Hz (n = 5 experiments with > 50 boutons for each). Traces were corrected for photobleaching. Error bars represent s.e.m. Scale bar, 5 μ m.

Figure 4. Readily retrievable surface pool of synaptic vesicle constituents.

(a) Cleaving membrane-stranded spH with TEV protease does not affect the cypHer signal at α Syt1-cypHer co-stained boutons. Average fluorescence responses to 50 APs at 20 Hz (n = 3 experiments with > 50 boutons for each). The spH fluorescence (black) shows little or no recovery, while the cypHer signal (gray) shows normal fluorescence recovery demonstrating endocytosis of vesicle constituents (Syt1) different from those freshly exocytosed. Error bars represent s.e.m.

(b,c) Photobleaching for 5 min at external pH 8.5 affects preferentially the vesicular pool of cypHer-tagged molecules. 50 APs at 20 Hz induced typical spH fluorescence transients (black, n = 5 experiments with > 50 boutons for each). However the cypHer signal (gray) for both (b) Syt1 and (c) VGAT increases in parallel to the spH decay indicating endocytosis of vesicle proteins from a readily retrievable pool (RRetP) resident on the bouton membrane. Error bars represent s.e.m.

(d,e) Average fluorescence profiles of boutons (n = 3 experiments with > 50 boutons for each) labeled with only α Syt1-cypHer (d) or α VGAT-cypHer (e). Experiments were performed as in panels (b and c), but using non-transfected neuronal cultures. This indicates that spH overexpression does not alter the dynamics or size of the RRetP. Error bars represent s.e.m.

(f) Comparison of RRP and RRetP sizes measured by different labeling strategies for Syt1 and VGAT. Prebleaching denotes the cypHer fluorescence decrease upon 50 APs at 20 Hz, a measure of the RRP size (40.2 ± 6.9 a.u. for Syt1 and 34.8 ± 3.6 a.u. for VGAT), postbleach the fluorescence increase (19.5 ± 6.2 a.u. for Syt1 and 17.7 ± 2.1 a.u. for VGAT) subsequent to vesicular cypHer bleaching upon 50 APs at 20 Hz (as shown in d and e). Surface staining denotes the fluorescence increase upon 50 APs at 20 Hz (53.7 ± 4.8 a.u.) after preferential labeling of the Syt1 surface pool (cf. Fig. 5a). Error bars represent s.e.m.

Figure 5. Repeated stimulation reveals reuse of the readily retrievable pool.

Average fluorescence profile of surface Syt1-labeled boutons (n = 3 experiments with > 50 boutons for each) stimulated first with 50 APs at 20 Hz followed by a second stimulation with either 50 (black) or 200 APs at 20 Hz (gray). In response to the second stimulus a marked fraction of SVs recycled from the RRetP upon the first stimulus is released. Error bars represent s.e.m.

Figure 6: Spatial organization of the readily retrievable pool.

3D dual-color isoSTED nanoscopy of cultured hippocampal boutons showing the localization of surface-stranded Syt1 (red) at synapses identified by the pre- and postsynaptic markers RIM1/2 and Homer1 (green), supported by 4Pi microscopy data of a large number of synapses.

(a) z-Projection of a 3D image stack of Syt1 at synapses labeled by RIM1/RIM2 as CAZ marker.

(b) z-Projection as in (a) of Syt1 at synapses labeled by Homer1 as PSD marker, with synapses at regions of interest numbered 1 to 3. Arrows mark the local orientation of the axon.

(c) Perspective views of volume rendered data. The Syt1 labeling reveals preassembled patches which are localized in the periphery of the active zone, i.e. typically within 500nm distance from the postsynaptic marker.

(d) Spatial distribution of Syt1 with respect to Homer1 for each region of interest (ROI). Histograms show Syt1-Homer1 cross-correlation, binned according to Syt1-Homer1 distance d and relative azimuth angle α which was measured with respect to the orientation of the axon as marked by arrows in (b). Distances between Syt1 patches and the postsynaptic marker accumulate at about 100-300 nm at angles where the probability to find Syt1 patches that are not associated with Homer1 is reduced (α deviating from 0 and $\pm \pi$).

(e) Nearest neighbor distances between Syt1 and RIM1/2 or Homer1 patches from dual color 4Pi microscopy stacks of n=74 (RIM1/2) and n=41 (Homer1) synapses. Insets show exemplary z-projections.

Scale bars, 1 μ m. Render volumes, 4.5 μ m x 7.0 μ m x 0.4 μ m full dataset, 1.5 μ m x 1.5 μ m x 0.4 μ m regions of interest 1 to 3.

ONLINE METHODS

Cell Culture

Primary cultures of rat hippocampal neurons were prepared from the CA3/CA1 region of 1 or 2 -day-old Wistar rats and transfected at 3 days in vitro (DIV) by a modified calcium phosphate transfection procedure¹³. Superecliptic pHluorin-synaptobrevin 2 (spH) was provided by G. Miesenböck (Department of Physiology, Anatomy and Genetics, Oxford University). For super-resolution microscopy Banker-type cultures of rat hippocampal neurons from P 1-3 d old Wistar rats were prepared and seeded on glass coverslips⁴⁸. All imaging experiments were carried out at 14-21 DIV.

TEV-protease cleavage

SpH-TEV transfected neurons were incubated with AcTEV protease and 1mM dithiothreitol (Invitrogen) for 15 min at room temperature as described previously¹³. After digestion, neurons were washed several times with normal Tyrode solution to remove the enzyme. Cleavage of the surface spH was observed over time as a reduction in the fluorescence signal.

Immunostaining

CypHer conjugated antibodies, α Syt1-cypHer and α VGAT-cypHer were used to label hippocampal neurons. Neurons were incubated with either α Syt1-cypHer or α VGAT-cypHer, at 37 °C for 3-4 hours in a carbonate buffer containing 120 mM NaCl, 5 mM KCl, 1 mM MgCl₂, 2.5 mM CaCl₂, 10 mM glucose and 18 mM NaHCO₃ ~pH 7.4. The cells were then washed twice and placed in a perfusion chamber containing modified Tyrode solution (150 mM NaCl, 4 mM KCl, 1 mM MgCl₂, 2 mM CaCl₂, 10 mM glucose, 10 mM HEPES buffer ~pH 7.4). Acidic buffer with final pH of 5.5 and 6.5 was prepared by replacing HEPES with MES, whereas alkaline solution with pH 8.5 and 9.5 was prepared by replacing HEPES with BICIN, all other components remained unchanged.

For pH titration measurements of cypHer, α Syt1-cypHer labeled neurons were stained, washed and then fixed with 4% paraformaldehyde (PFA). Cells were permeabilized with 0.4% saponin to make the internalized antibodies accessible to perfusion with buffers of differing pH. The surface pool staining for **Fig. 4f** and **Fig. 5** were performed by incubating the neurons with saturating concentrations of α Syt1-cypHer in presence of 0.5 μ M TTX for 5 min at room temperature. The neurons were then washed with normal Tyrode solution and used for imaging.

To label the surface fraction of Syt1 for super-resolution microscopy, live hippocampal neurons on coverslips were washed 3 times in Ca^{2+} free solution (120mM NaCl, 5mM KCl, 3.5mM MgCl_2 , 10mM D-glucose, 10mM HEPES and 1mM EGTA) containing 0.5 μ M TTX and incubated with the synaptotagmin 1 mouse monoclonal antibody (604.1; 1:10 cell culture supernatant; Synaptic Systems) and 2% goat serum for 45 min at 4 degree. After 3 wash steps cells were fixed for 10 min at room temperature (RT) in 4% PFA and washed again 4 times for 3 min. For labelling the total fraction of Homer1 or RIM1/2 cells were permeabilized and simultaneously blocked with buffer containing 2% goat serum, 1% BSA and 0.4% saponin for 15 min. Subsequently, coverslips were incubated for 1 hr at RT with a rabbit polyclonal Homer1 or RIM1/2 (Zn-finger domain) antibody (1:100; Synaptic Systems) using the same buffer conditions as for blocking. After washing 4 times for 3 min secondary antibodies labelled with KK114 (1:100) and DY-480XL (1:100, Dyomics GmbH) and Alexa 488 (1:100; Invitrogen) and Alexa 594 (1:100; Invitrogen) for isoSTED and 4Pi microscopy respectively were applied and incubated for 1 hr at RT. After 4 final wash steps for 3 min coverslips were mounted and used for isoSTED and 4Pi microscopy respectively.

Epifluorescence microscopy

Synaptic boutons were stimulated by electric field stimulation (platinum electrodes 10-mm spacing, 1 ms pulses of 50 mA and alternating polarity) were applied by constant current stimulus isolator (WPI A 385, World Precision Instruments); 10 mM 6-cyano-7-nitroquinoxaline-2, 3-dione (CNQX) and 50 mM D, L-2-amino-5-phosphonovaleric acid (AP5) were added to prevent recurrent activity. Fast solution exchanges

were achieved through a two-barrel glass tubing perfusion system controlled by a piezo-controlled stepper device (SF778, Warner Instruments).

Image acquisition for experiments in **Figs. 1e-f, 2, 3, and Supplementary Fig. 1** were performed at RT by a cooled slow-scan CCD camera (SensiCam-QE, PCO) mounted on an inverted microscope (Axiovert S100TV, Zeiss) with a 63x, 1.2 NA water-immersion objective and an FITC/Cy5 dual-band filter set (AHF analysentechnik AG). spH and cypHer were excited at 480 nm and 640 nm, respectively with a computer-controlled monochromator (Polychrom II, Till Photonics). Time lapse images of spH (green) and cypHer (red) were acquired at 0.5 Hz alternately. For all other experiments concerning RRetP visualization, from **Fig. 4** onwards, an electron multiplying charge couple device (EM-CCD) was used (Andor iXon+ DU-897E-BV camera; Andor Technology) controlled by Andor iQ Software (Andor Technology) and mounted on an inverted Nikon TE2000 microscope equipped with a 60x, 1.2 NA water-immersion objective and an FITC/Cy5 dual-band filter set (AHF analysentechnik AG). Vesicular cypHer was photobleached by continuous exposure to red light (640 nm) for 5 min. During the cypHer bleaching procedure, cells were bathed in an alkaline buffer solution of pH 8.5 for better protection of surface bound cypHer molecules.

Images were analyzed using self-written routines in Matlab (MathWorks). Active boutons were localized based on spH fluorescence using an automated routine where a difference image is generated by subtracting an average of five frames before from after stimulation. Spots on the difference image, each representing a putative functional bouton, were identified and centered based on the maximum pixel intensity. Only spots with fluorescence response $> 2\sigma$ of baseline fluorescence were chosen for analysis. Square regions of interest (ROI, $1.5 \times 1.5 \mu\text{m}^2$) were centered on these spots in both the spH and cypHer channel and average fluorescence profiles were then plotted. Due to low transfection efficiency of spH, not every cypHer positive bouton was spH positive. For dual-color recordings, we used the co-ordinates of the ROIs identified from spH response to define the positions of active boutons in the cypHer channel. Fluorescence traces from individual boutons were normalized before calculating the average response.

As the cypHer fluorophore displays much less photo-stability compared to its prototype (Cyanine 5 dye), in some of the initial experiments not using an EM-CCD the intensity of time-lapse images was corrected for

820 nm. The beam expander was set to 3 or 6. Fluorescence originating from the sample was passed through a filter cube (SP700, BS560, BP500–550, and BP607–683), and its intensity was measured by photon counting avalanche photodiodes (PerkinElmer). The detection pinhole was set to 0.86 Airy units. Samples were mounted between the two objectives, and focus and phase of the counter-propagating beams were pre-aligned to the immobilized beads. Then stacks of the cells were recorded with a pixel size between $10 \times 10 \text{ nm}^2$ and $18 \times 18 \text{ nm}^2$ in xz –direction. The step size in y-direction was 97 nm with water immersion lenses and 61 nm with oil immersion lenses, respectively.

4Pi raw images were linearly brightened, rescaled, and linearly filtered by a subresolution mask employing the image processing program ImageJ (Wayne Rasband, National Institutes of Health, <http://rsb.info.nih.gov/ij>).

A detailed description of 4Pi distance analysis has been published recently²². Briefly, the intensity profiles of the PSF's main maximum in the two detection channels were independently fitted to an elliptical 2D gaussian function using a commercial plugin for Image J (ILTracker, Ingo Lepper Software/Consulting) and the distance between the two centers was calculated.

For the distance analysis only the nearest neighbors were taken into account. Additionally, for the RIM1/2 and Syt1 double staining, only patches that were diffraction limited in the red channel were analyzed.

Dual-color isoSTED imaging in the far-red

For isoSTED imaging, the PBS buffer was exchanged by a dilution series with TDE (2,2'-thiodiethanol) in PBS⁴⁹, finally resulting in an embedding medium of 97% (v/v) TDE in PBS. The sample was covered with a second cover slip that was sparsely coated with fluorescent beads (Crimson fluorescent microspheres, specified diameter: 100 nm; Molecular Probes) to facilitate the initial alignment of the isoSTED nanoscope. Excitation of the dyes DY-480XL and KK114 was performed sequentially at a wavelength of 530 nm and 635 nm respectively, utilizing pulsed semiconductor lasers (PicoTA 530 and LDH-P-C 635b, each with PDL 800-B, PicoQuant) delivering <100 ps excitation pulses. These were synchronized with ~300 ps STED pulses originating from a mode-locked Titanium:Sapphire laser (Mai Tai, Spectra-Physics GmbH)

operating at 79 MHz and at a wavelength of 775 nm, delivered and stretched by a single-mode optical fiber. Depending on laser availability, the fiber coupled Titanium:Sapphire setup was replaced with a frequency doubled fiber laser (ELP-5-775-DG, IPG Photonics Corporation) that emits 1 ns long pulses at 20 MHz and at the same wavelength. In both cases, the time-averaged STED power in the sample was about 50 mW. Detection of the emission of both types of fluorophores was carried out in the 660–700 nm wavelength range using a photon-counting avalanche photodiode (APD) (PerkinElmer) and recorded in separate channels. 3D dual-color image stacks of synapses were non-linearly deconvolved by applying 20 iterations of a Richardson-Lucy algorithm⁵⁰ to account for blurring effects of the imaging system. To this end, PSF estimates for both channels (DY-480XL and KK114) were obtained from the images of respective dye-tagged antibody clusters in remote areas of the sample. In case of the Syt1-RIM1/2 measurement, all signal within 60nm distance to the coverslip was discarded in order to reduce the contribution of non specifically bound antibodies to the analysis.

Analysis of the spatial distribution of Syt1 vs. Homer1

Correlation analysis was performed in Matlab independently on each of the marked regions (**Fig. 6b**) and evaluated in radial coordinates (d, θ) with $d = \sqrt{dx^2 + dy^2 + dz^2}$ denoting the distance and $\theta = \text{atan2}(dx, dy)$ denoting the azimuth angle between voxels. In order to estimate the orientation of the axon, the azimuth direction θ_{hom} of the local Homer1 run was obtained from the smoothed Homer1 intensity auto-correlation $H_{sm}(d, \theta)$ as $\theta_0 := \text{argmax}(\sum_d H_{sm}(d, \theta))$ and represented by an arrow within the respective region (**Fig. 6b**). Subsequently, the Syt1-Homer1 cross-correlation $S(d, \theta)$ was calculated, taking into account all data values that exceeded a 10% lower threshold with regard to the global maximum. The result was transformed according to $S(d, \theta) \mapsto S(d, \alpha)$ with $\alpha = \theta - \theta_0$, and finally binned into a histogram (**Fig. 6d**).

References

1. Heuser, J.E. & Reese, T.S. Evidence for recycling of synaptic vesicle membrane during transmitter release at the frog neuromuscular junction. *J Cell Biol* **57**, 315-344 (1973).
2. Granseth, B., Odermatt, B., Royle, S.J. & Lagnado, L. Clathrin-mediated endocytosis is the dominant mechanism of vesicle retrieval at hippocampal synapses. *Neuron* **51**, 773-786 (2006).
3. Mueller, V.J., Wienisch, M., Nehring, R.B. & Klingauf, J. Monitoring clathrin-mediated endocytosis during synaptic activity. *J Neurosci* **24**, 2004-2012 (2004).
4. Wu, L.G., Ryan, T.A. & Lagnado, L. Modes of vesicle retrieval at ribbon synapses, calyx-type synapses, and small central synapses. *J Neurosci* **27**, 11793-11802 (2007).
5. He, L., Wu, X.S., Mohan, R. & Wu, L.G. Two modes of fusion pore opening revealed by cell-attached recordings at a synapse. *Nature* **444**, 102-105 (2006).
6. Zhang, Q., Li, Y. & Tsien, R.W. The dynamic control of kiss-and-run and vesicular reuse probed with single nanoparticles. *Science* **323**, 1448-1453 (2009).
7. Ceccarelli, B., Hurlbut, W.P. & Mauro, A. Turnover of transmitter and synaptic vesicles at the frog neuromuscular junction. *J Cell Biol* **57**, 499-524 (1973).
8. Gandhi, S.P. & Stevens, C.F. Three modes of synaptic vesicular recycling revealed by single-vesicle imaging. *Nature* **423**, 607-613 (2003).
9. Koenig, J.H., Yamaoka, K. & Ikeda, K. Omega images at the active zone may be endocytotic rather than exocytotic: implications for the vesicle hypothesis of transmitter release. *Proc Natl Acad Sci U S A* **95**, 12677-12682 (1998).
10. Miesenbock, G., De Angelis, D.A. & Rothman, J.E. Visualizing secretion and synaptic transmission with pH-sensitive green fluorescent proteins. *Nature* **394**, 192-195 (1998).
11. Fernandez-Alfonso, T., Kwan, R. & Ryan, T.A. Synaptic vesicles interchange their membrane proteins with a large surface reservoir during recycling. *Neuron* **51**, 179-186 (2006).
12. Dittman, J.S. & Kaplan, J.M. Factors regulating the abundance and localization of synaptobrevin in the plasma membrane. *Proc Natl Acad Sci U S A* **103**, 11399-11404 (2006).
13. Wienisch, M. & Klingauf, J. Vesicular proteins exocytosed and subsequently retrieved by compensatory endocytosis are nonidentical. *Nat Neurosci* **9**, 1019-1027 (2006).
14. Teng, H., Cole, J.C., Roberts, R.L. & Wilkinson, R.S. Endocytic active zones: hot spots for endocytosis in vertebrate neuromuscular terminals. *J Neurosci* **19**, 4855-4866 (1999).
15. Teng, H. & Wilkinson, R.S. Clathrin-mediated endocytosis near active zones in snake motor boutons. *J Neurosci* **20**, 7986-7993 (2000).

16. Taubenblatt, P., Dedieu, J.C., Gulik-Krzywicki, T. & Morel, N. VAMP (synaptobrevin) is present in the plasma membrane of nerve terminals. *J Cell Sci* **112** (Pt 20), 3559-3567 (1999).
17. Willig, K.I., Rizzoli, S.O., Westphal, V., Jahn, R. & Hell, S.W. STED microscopy reveals that synaptotagmin remains clustered after synaptic vesicle exocytosis. *Nature* **440**, 935-939 (2006).
18. Miller, T.M. & Heuser, J.E. Endocytosis of synaptic vesicle membrane at the frog neuromuscular junction. *J Cell Biol* **98**, 685-698 (1984).
19. Balaji, J. & Ryan, T.A. Single-vesicle imaging reveals that synaptic vesicle exocytosis and endocytosis are coupled by a single stochastic mode. *Proc Natl Acad Sci U S A* **104**, 20576-20581 (2007).
20. Adie, E.J., *et al.* CypHer 5: a generic approach for measuring the activation and trafficking of G protein-coupled receptors in live cells. *Assay Drug Dev Technol* **1**, 251-259 (2003).
21. Martens, H., *et al.* Unique luminal localization of VGAT-C terminus allows for selective labeling of active cortical GABAergic synapses. *J Neurosci* **28**, 13125-13131 (2008).
22. Huve, J., Wesselmann, R., Kahms, M. & Peters, R. 4Pi microscopy of the nuclear pore complex. *Biophys J* **95**, 877-885 (2008).
23. Kano, H., Jakobs, S., Nagomi, M. & Hell, S.W. Dual-color 4Pi-confocal microscopy with 3D-resolution in the 100 nm range. *Ultramicroscopy* **90**, 207-213 (2001).
24. Schmidt, R., *et al.* Spherical nanosized focal spot unravels the interior of cells. *Nat Methods* **5**, 539-544 (2008).
25. Roos, J. & Kelly, R.B. The endocytic machinery in nerve terminals surrounds sites of exocytosis. *Curr Biol* **9**, 1411-1414 (1999).
26. Shupliakov, O., *et al.* Impaired recycling of synaptic vesicles after acute perturbation of the presynaptic actin cytoskeleton. *Proc Natl Acad Sci U S A* **99**, 14476-14481 (2002).
27. Gundelfinger, E.D., Kessels, M.M. & Qualmann, B. Temporal and spatial coordination of exocytosis and endocytosis. *Nat Rev Mol Cell Biol* **4**, 127-139 (2003).
28. Sankaranarayanan, S., De Angelis, D., Rothman, J.E. & Ryan, T.A. The use of pHluorins for optical measurements of presynaptic activity. *Biophys J* **79**, 2199-2208 (2000).
29. Sankaranarayanan, S. & Ryan, T.A. Real-time measurements of vesicle-SNARE recycling in synapses of the central nervous system. *Nat Cell Biol* **2**, 197-204 (2000).
30. Fernandez-Alfonso, T. & Ryan, T.A. The kinetics of synaptic vesicle pool depletion at CNS synaptic terminals. *Neuron* **41**, 943-953 (2004).
31. Schikorski, T. & Stevens, C.F. Quantitative ultrastructural analysis of hippocampal excitatory synapses. *J Neurosci* **17**, 5858-5867 (1997).
32. Murthy, V.N. & Stevens, C.F. Reversal of synaptic vesicle docking at central synapses. *Nat Neurosci* **2**, 503-507 (1999).
33. Schikorski, T. & Stevens, C.F. Morphological correlates of functionally defined synaptic vesicle populations. *Nat Neurosci* **4**, 391-395 (2001).

34. Tabares, L., *et al.* Monitoring synaptic function at the neuromuscular junction of a mouse expressing synaptopHluorin. *J Neurosci* **27**, 5422-5430 (2007).
35. Takamori, S., *et al.* Molecular anatomy of a trafficking organelle. *Cell* **127**, 831-846 (2006).
36. Vanden Berghe, P. & Klingauf, J. Synaptic vesicles in rat hippocampal boutons recycle to different pools in a use-dependent fashion. *J Physiol* **572**, 707-720 (2006).
37. Staras, K., *et al.* A vesicle superpool spans multiple presynaptic terminals in hippocampal neurons. *Neuron* **66**, 37-44 (2010).
38. Fredj, N.B. & Burrone, J. A resting pool of vesicles is responsible for spontaneous vesicle fusion at the synapse. *Nat Neurosci* **12**, 751-758 (2009).
39. Groemer, T.W. & Klingauf, J. Synaptic vesicles recycling spontaneously and during activity belong to the same vesicle pool. *Nat Neurosci* **10**, 145-147 (2007).
40. Sara, Y., Virmani, T., Deak, F., Liu, X. & Kavalali, E.T. An isolated pool of vesicles recycles at rest and drives spontaneous neurotransmission. *Neuron* **45**, 563-573 (2005).
41. Hua, Y., Sinha, R., Martineau, M., Kahms, M. & Klingauf, J. A common origin of synaptic vesicles undergoing evoked and spontaneous fusion. *Nat Neurosci* **13**, 1451-1453 (2010).
42. Brodin, L. & Shupliakov, O. Giant reticulospinal synapse in lamprey: molecular links between active and periaxonal zones. *Cell Tissue Res* **326**, 301-310 (2006).
43. Kim, S.H. & Ryan, T.A. Synaptic vesicle recycling at CNS synapses without AP-2. *J Neurosci* **29**, 3865-3874 (2009).
44. Glyvuk, N., *et al.* AP-1/sigma1B-adaptin mediates endosomal synaptic vesicle recycling, learning and memory. *EMBO J* **29**, 1318-1330 (2010).
45. Hosoi, N., Holt, M. & Sakaba, T. Calcium dependence of exo- and endocytotic coupling at a glutamatergic synapse. *Neuron* **63**, 216-229 (2009).
46. Wu, X.S., *et al.* Ca²⁺ and calmodulin initiate all forms of endocytosis during depolarization at a nerve terminal. *Nat Neurosci* **12**, 1003-1010 (2009).
47. Yao, C.K., *et al.* A synaptic vesicle-associated Ca²⁺ channel promotes endocytosis and couples exocytosis to endocytosis. *Cell* **138**, 947-960 (2009).
48. Goslin, K. & Banker, G. Rat Hippocampal Neurons in Low-Density Culture. in *Culturing Nerve Cells 1st edn.* (ed. G. Banker & K. Goslin) 251-281 (MIT Press, Cambridge, 1991).
49. Staudt, T., Lang, M.C., Medda, R., Engelhardt, J. & Hell, S.W. 2,2'-thiodiethanol: a new water soluble mounting medium for high resolution optical microscopy. *Microsc Res Tech* **70**, 1-9 (2007).
50. Richardson, W.H. Bayesian-based iterative method of image restoration. *J. Opt. Soc. Am.* **62**, 55-59 (1972).

SI Guide

Supplementary Figure 1. Comparison of α Syt1-cypHer uptake for labeling of boutons by evoked and spontaneous activity.

Supplementary Figure 2. Data analysis of cypHer & spH dual-color measurements.

Supplementary Figure 3. Retrieval of freshly exocytosed material upon depletion of the RRetP.

Supplementary Figure 4. Antigen accessibility for antibodies in the synaptic cleft measured with 4Pi microscopy.

Supplementary Figure 5. Azimuthal angle analysis of Syt1 vs. Homer1 patches in 4Pi microscopy image stacks.

Supplementary Information Titles

Please list each supplementary item and its title or caption, in the order shown below. Please include this form at the end of the Word document of your manuscript or submit it as a separate file.

Note that we do NOT copy edit or otherwise change supplementary information, and minor (nonfactual) errors in these documents cannot be corrected after publication. Please submit document(s) exactly as you want them to appear, with all text, images, legends and references in the desired order, and check carefully for errors.

Journal: Nature Neuroscience

Article Title:	A readily retrievable pool of synaptic vesicles
Corresponding Author:	Jurgen Klingauf klingauf@uni-muenster.de
	Dept. of Cellular Biophysics, Institute of Medical Physics and Biophysics, University of Muenster, Robert-Koch-Str. 31, 48149 Muenster, Germany

Supplementary Item & Number (add rows as necessary)	A readily retrievable pool of synaptic vesicles
Supplementary Figure 1	Comparison of α Syt1-cypHer uptake for labeling of boutons by evoked and spontaneous activity.
Supplementary Figure 2	Data analysis of cypHer & spH dual-color measurements.
Supplementary Figure 3	Retrieval of freshly exocytosed material upon depletion of the RRetP.
Supplementary Figure 4	Antigen accessibility for antibodies in the synaptic cleft measured with 4Pi microscopy.
Supplementary Figure 5	Azimuthal angle analysis of Syt1 vs. Homer1 patches in 4Pi microscopy image stacks.
Supplementary Table 1	[TITLE OF TABLE (descriptive title)]
Supplementary Methods (or Discussion or Data or Note)	[NO DESCRIPTIVE TITLE NECESSARY]
Supplementary Video 1 (or Audio or Spreadsheet)	[CAPTION TO BE POSTED ONLINE (include title and explanation of contents)]

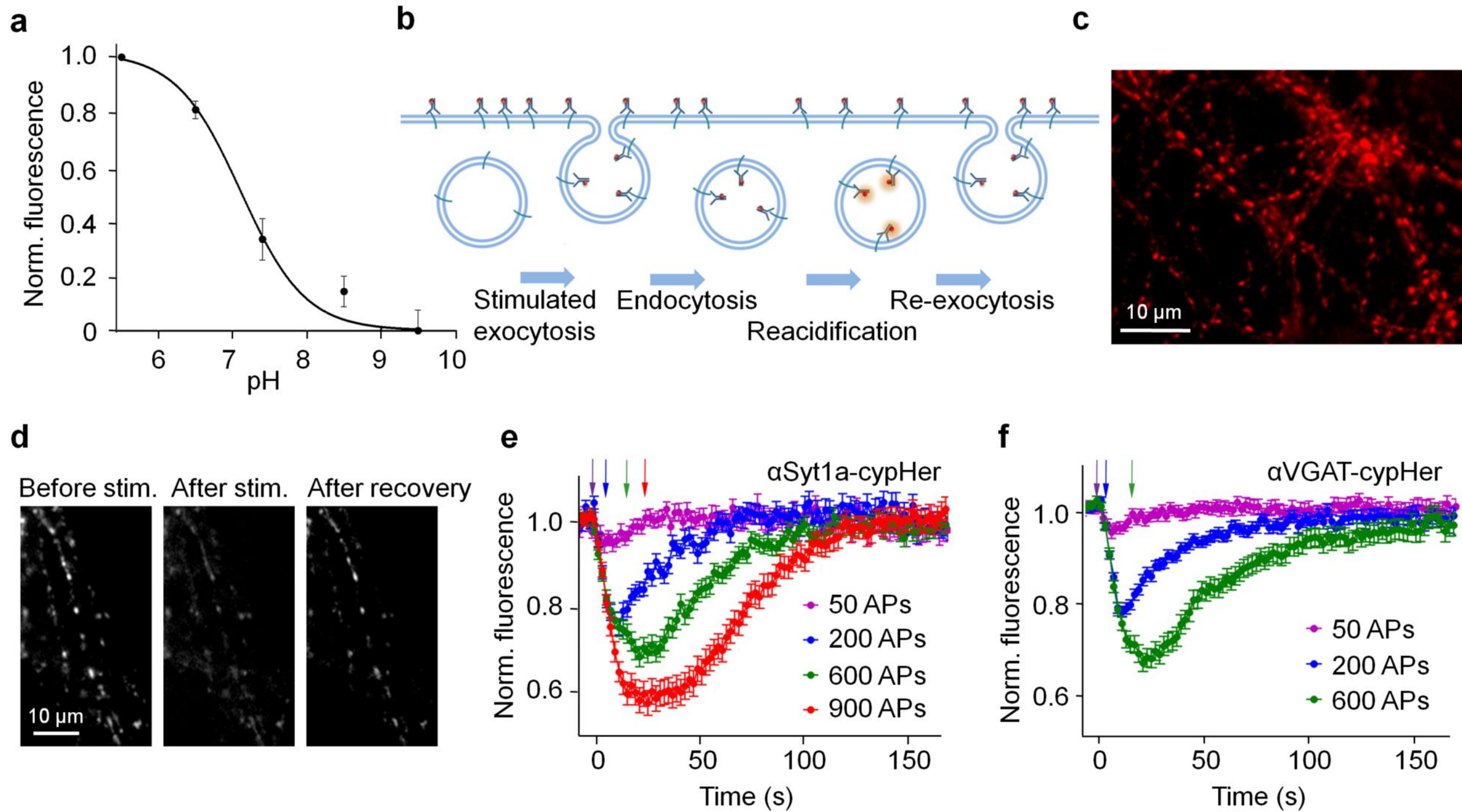


Figure 1

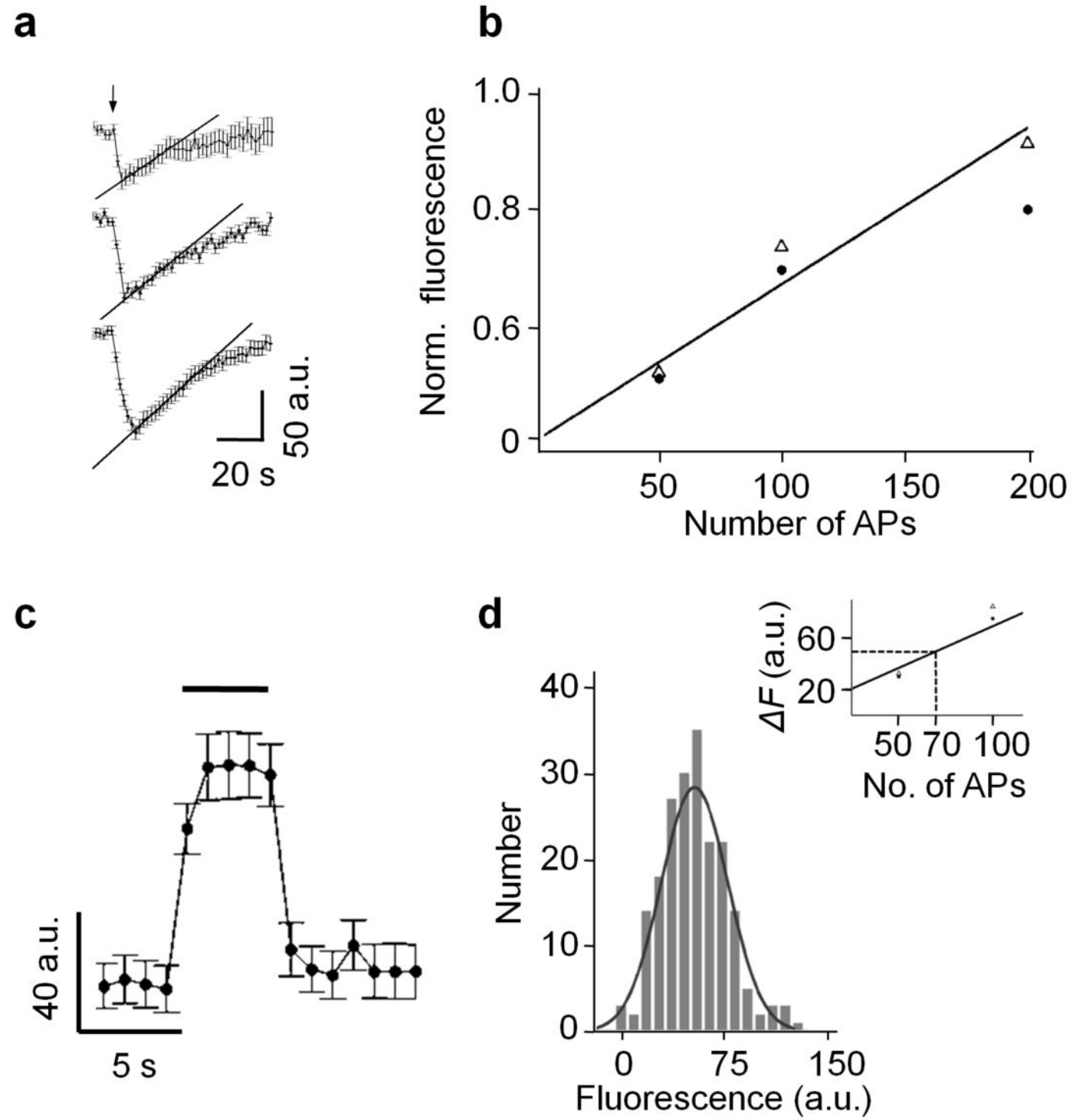


Figure 2

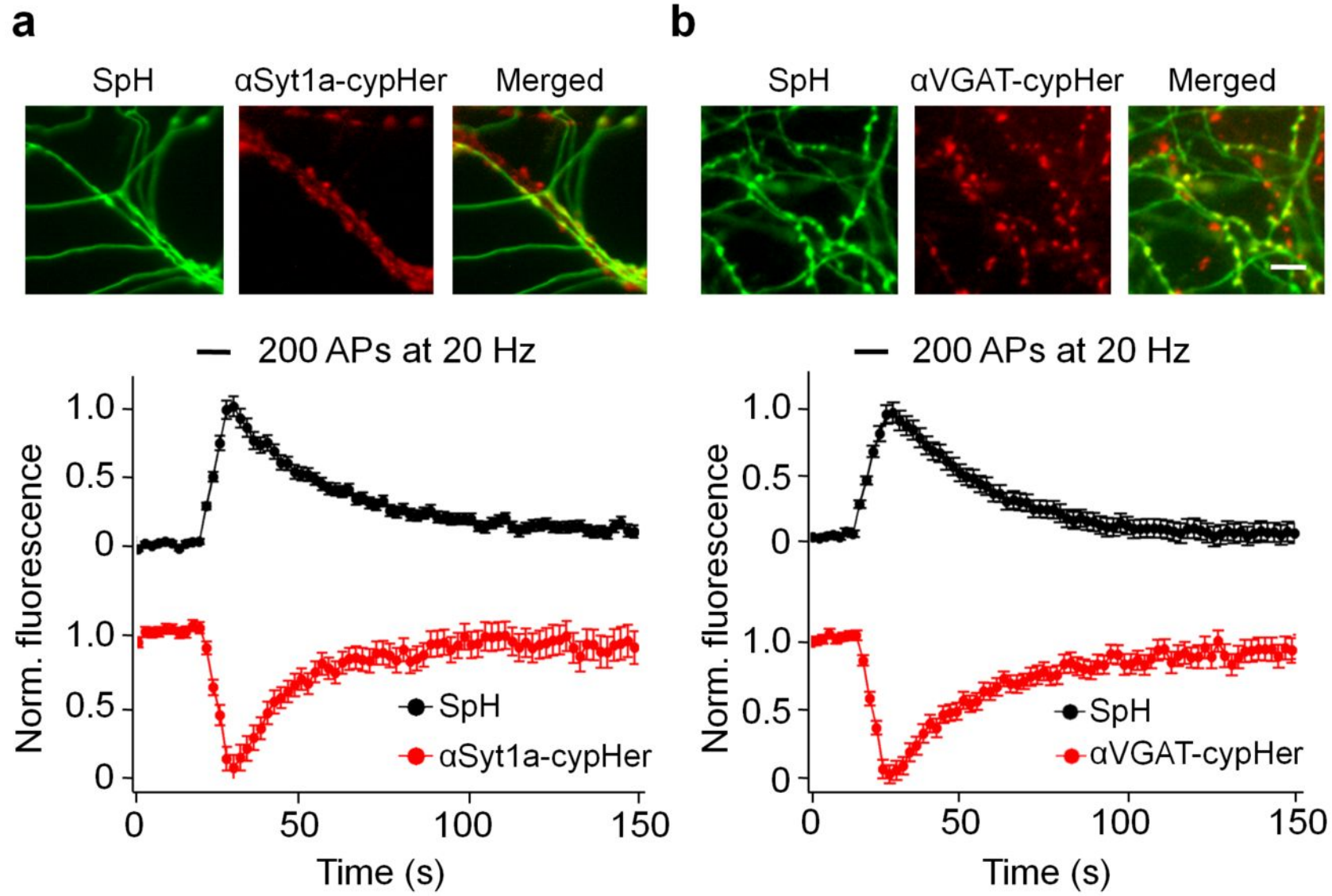


Figure 3

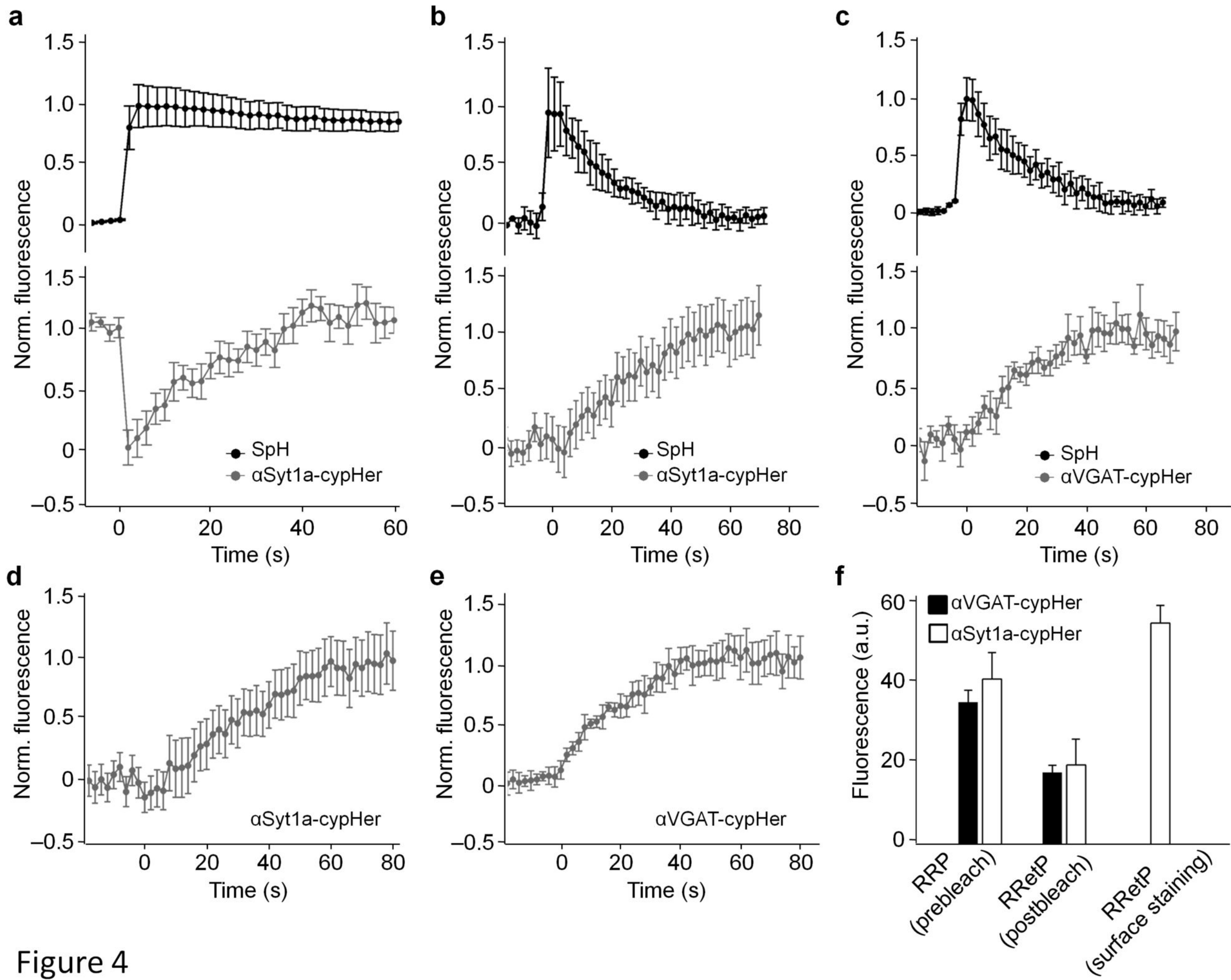


Figure 4

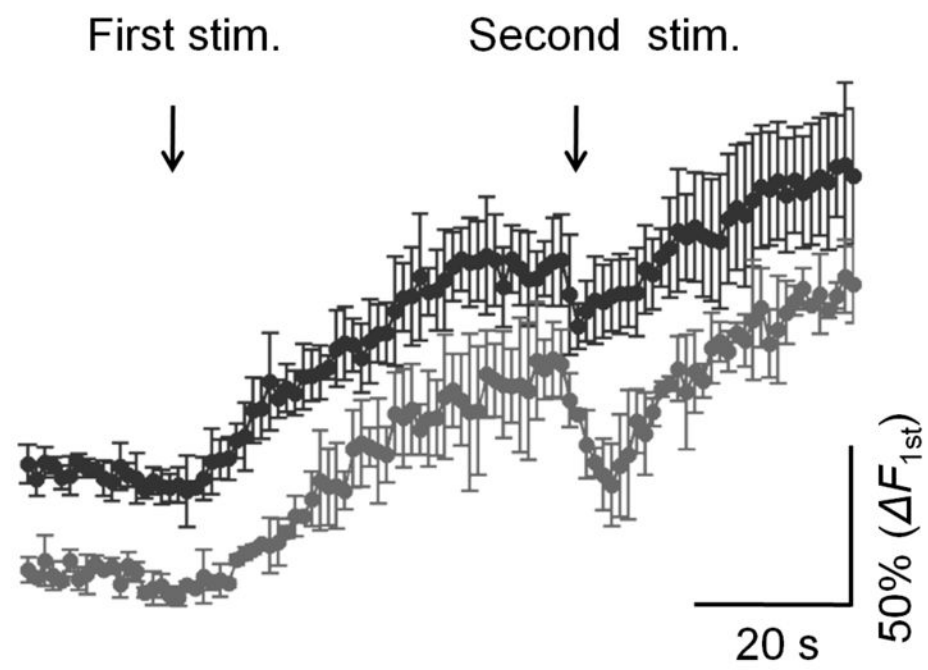
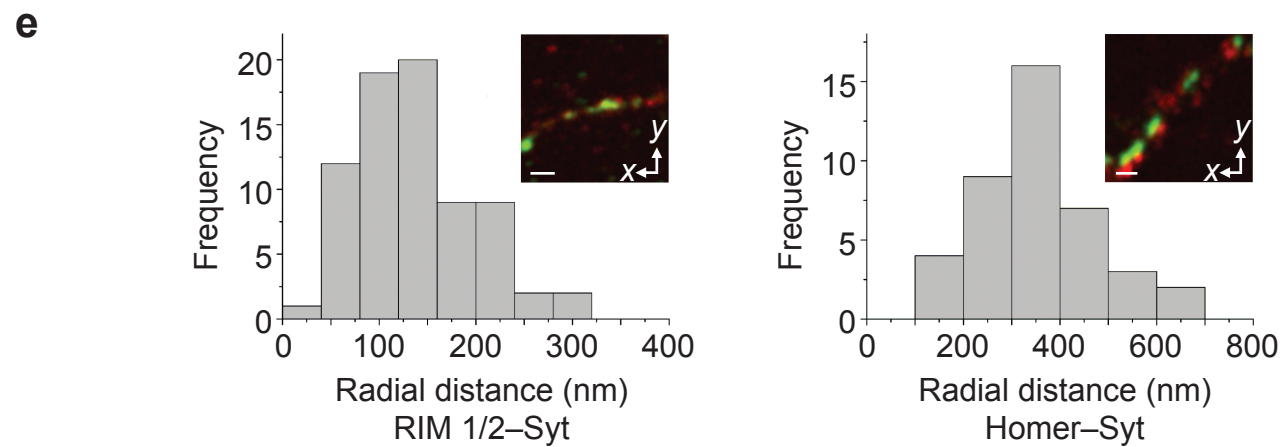
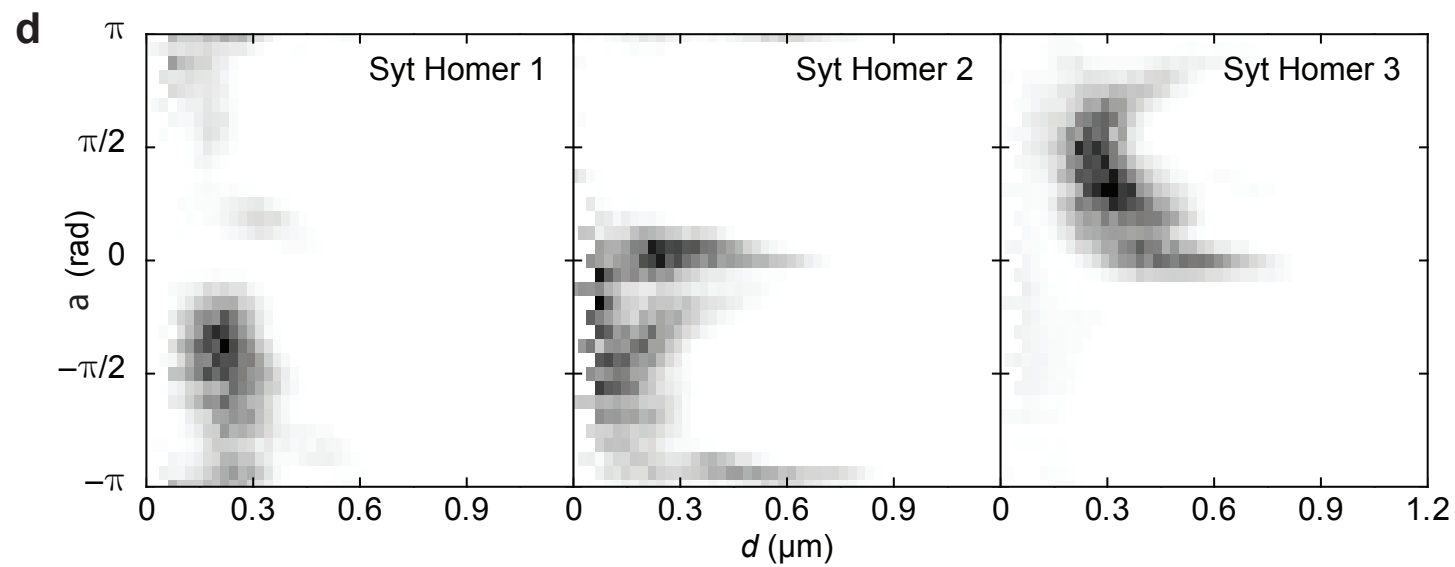
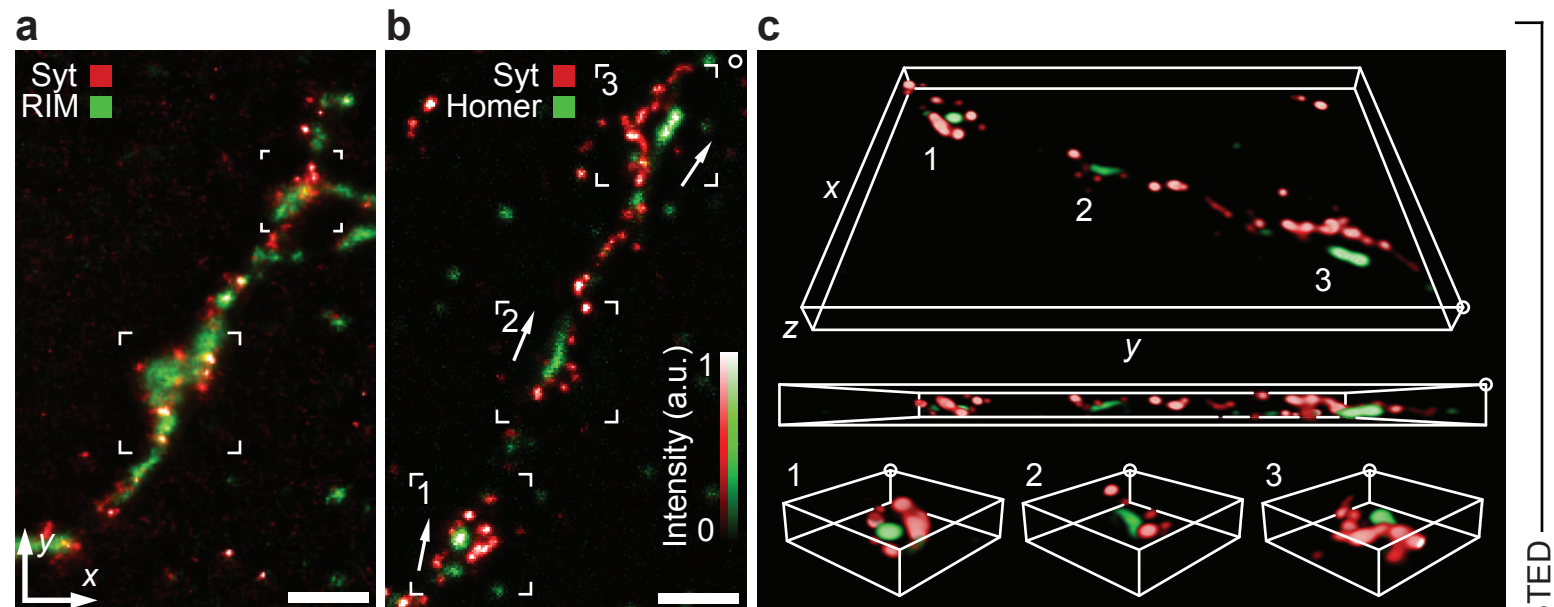


Figure 5



isoSTED

4Pi